Biogenesis of the bacterial cbb_3 cytochrome *c* oxidase: Active subcomplexes support a sequential assembly model

Received for publication, July 3, 2017, and in revised form, October 30, 2017 Published, Papers in Press, November 17, 2017, DOI 10.1074/jbc.M117.805184

Anne Durand[1], Marie-Line Bourbon, Anne-Soisig Steunou, Bahia Khalfaoui-Hassani[2], Camille Legrand, Audrey Guitton, Chantal Astier, and Soufian Ouchane[3]

From the Institute for Integrative Biology of the Cell (I2BC), Commissariat à l'Énergie Atomique, CNRS, Université Paris-Sud, Université Paris-Saclay, 91198 Gif sur Yvette Cedex, France

Edited by Karen G. Fleming

The cbb_3 oxidase has a high affinity for oxygen and is required for growth of bacteria, including pathogens, in oxygen-limited environments. However, the assembly of this oxidase is poorly understood. Most cbb_3 are composed of four subunits: the catalytic CcoN subunit, the two cytochrome *c* subunits (CcoO and CcoP) involved in electron transfer, and the small CcoQ subunit with an unclear function. Here, we address the role of these four subunits in cbb_3 biogenesis in the purple bacterium *Rubrivivax gelatinosus*. Analyses of membrane proteins from different mutants revealed the presence of active CcoNQO and CcoNO subcomplexes and also showed that the CcoP subunit is not essential for their assembly. However, CcoP was required for the oxygen reduction activity in the absence of CcoQ. We also found that CcoQ is dispensable for forming an active CcoNOP subcomplex in membranes. CcoNOP exhibited oxygen reductase activity, indicating that the cofactors (hemes *b* and copper for CcoN and cytochromes *c* for CcoO and CcoP) were present within the subunits. Finally, we discovered the presence of a CcoNQ subcomplex and showed that CcoN is the required anchor for the assembly of the full CcoNQOP complex. On the basis of these findings, we propose a sequential assembly model in which the CcoQ subunit is required for the early maturation step: CcoQ first associates with CcoN before the CcoNQ–CcoO interaction. CcoP associates to CcoNQO subcomplex in the late maturation step, and once the CcoNQOP complex is fully formed, CcoQ is released for degradation by the FtsH protease. This model could be conserved in other bacteria, including the pathogenic bacteria lacking the assembly factor CcoH as in *R. gelatinosus*.

cbb_3 cytochrome *c* oxidases (Cox)[4] belong to the *c*-type heme-copper oxidase family and use *c*-type cytochromes as electron donors. They are restricted to bacteria, and in the case of several pathogens, cbb_3-Cox is the only terminal oxidase of the respiratory electron transfer chain (1–4). In addition to O_2 reduction and proton pumping across the inner membrane, cbb_3-Cox oxygen reductase activity is also required to initiate other metabolic pathways that are often associated with growth under microaerobic conditions such as nitrogen fixation in *Bradyrhizobium japonicum* (5, 6) and photosynthesis in *Rubrivivax gelatinosus* (7) and *Rhodobacter sphaeroides* (8). Furthermore, cbb_3-Cox of various human and plant bacterial pathogens were proposed to be involved in colonization of anoxic tissues (4, 9–11).

Given its prominent role in pathogenic bacterial survival in a hypoxic environment, cbb_3-Cox therefore represents an interesting target to limit their growth and development. Most cbb_3-Cox are four-subunit integral membrane complexes containing various cofactors required for the enzyme activity. In the X-ray structure of *Pseudomonas stutzeri* cbb_3-Cox, three of these conserved subunits (CcoN, CcoO, and CcoP) are present with a fourth subunit, CcoM, specific to the genus *Pseudomonas* (12, 13). CcoN, the catalytic subunit, is a 12-membrane-spanning helix protein containing a low-spin *b* heme, a high-spin b_3-Cu_B binuclear center, and a calcium ion. CcoO is composed of one N-terminal transmembrane helix and a periplasmic soluble monoheme *c*-type cytochrome. CcoP is anchored in the membrane via two N-terminal transmembrane helices and contains a large periplasmic diheme *c*-type cytochrome. In other bacteria, CcoQ is the fourth subunit with a single transmembrane helix (14–16). CcoQ is not essential for the cbb_3-Cox activity in *B. japonicum* (17) and *Rhodobacter capsulatus* (18) and was also suggested to stabilize the cbb_3-Cox in *R. sphaeroides* (15). Likewise, in *P. stutzeri*, CcoQ (19) and CcoM were recently proposed to be involved in the assembly and/or stability of cbb_3 complex (13, 19). In *Pseudomonas aeruginosa*, two copies of *ccoO* and *ccoP* and up to four different *ccoN* and *ccoQ* genes were identified. Interestingly, the bacterium can produce multiple cbb_3 isoforms through exchanges of multiple core catalytic subcomplexes (20).

Although it is well established that CcoN, CcoO, and CcoP are required for oxygen reduction activity (17, 21), the requirement of each subunit for the assembly of the Cox complex is less consensual. In *B. japonicum*, almost wild-type levels of FixN (CcoN) and FixO (CcoO) were found in a *fixP* (*ccoP*) insertion mutant (17). In contrast with *R. capsulatus ccoP*$^-$ mutants,

This work was supported by Agence Nationale de la Recherche Grant BLAN06-2_147814. The authors declare that they have no conflicts of interest with the contents of this article.

This article contains Figs. S1–S3.

[1] To whom correspondence may be addressed: CNRS, I2BC, UMR9198, F-91198 Gif sur Yvette, France. Tel.: 33-1-69-82-31-65; Fax: 33-1-69-82-32-30; E-mail: anne.durand@i2bc.paris-saclay.fr.

[2] Present address: Dept. of Biology, University of Pennsylvania, 433 S. University Ave., Philadelphia, PA 19104.

[3] To whom correspondence may be addressed: CNRS, I2BC, UMR9198, F-91198 Gif sur Yvette, France. Tel.: 33-1-69-82-31-65; Fax: 33-1-69-82-32-30; E-mail: soufian.ouchane@i2bc.paris-saclay.fr.

[4] The abbreviations used are: Cox, cytochrome *c* oxidase(s); BN, blue native; DAB, 3,3′-diaminobenzidine tetrahydrochloride; ANOVA, analysis of variance.

CcoN and CcoO were absent on Western blots (21); however, CcoN was recently detected in the absence of both CcoO and CcoP (22). Similarly, CcoN and CcoP were not detected in *B. japonicum ccoO*$^-$ mutant (17, 23). In *R. capsulatus ccoO*$^-$ mutant, CcoN and CcoP were not detected (21) until recently upon reexamination of the mutant in which CcoN was finally identified (22). In both bacteria, however, CcoN is required for the presence of CcoO and CcoP (17, 21). CcoQ has not been reported so far in any of the single mutants described above. Although some of the assembly factors (CcoGHIS) have been identified (24), the assembly sequence of the individual subunits has not been completely established yet. So far, two subcomplexes, CcoNOH and CcoPQH, were identified in *R. capsulatus*, and CcoH was proposed to facilitate the assembly of these two modules. CcoI was shown to be required for copper insertion in the oxidase (24). In *B. japonicum*, FixN and FixO were suggested to be first inserted into the membrane and then form together a FixNO core complex independently of FixP. However, no direct evidence supported the presence of this FixNO subcomplex, and whether FixH and FixQ were associated within this complex was not addressed (17). The cbb_3-Cox biogenesis sequence is apparently similar but still incomplete in these two α-proteobacteria, and the proposed model is probably not conserved among all bacterial cbb_3-Cox. Indeed, this model is challenged in bacteria containing cbb_3-Cox and lacking the *ccoH* gene (25) like many pathogenic bacteria such as *Helicobacter pylori*, *Campylobacter jejuni*, and *Neisseria meningitidis*.

The purple photosynthetic bacterium *R. gelatinosus* can grow aerobically due to two terminal oxidases: the *bd* quinol oxidase and the cbb_3-Cox encoded by the *cydBA* and *ccoNQOP* operons, respectively (7). We have isolated single mutants (*ccoN*$^-$ and *ccoO*$^-$), but the presence of cbb_3 subcomplexes and other subunits in the membrane was not investigated (7, 25). In this work, we show that cbb_3-Cox undergoes a sequential assembly different from the modular model described for *R. capsulatus* (14, 26) involving CcoH. To increase our understanding of the cbb_3-Cox assembly steps, the contribution of each individual subunit to the assembly sequence was analyzed in the wild-type (WT) and mutants of *R. gelatinosus* by monitoring (i) the *in vivo* oxygen consumption under microaerobiosis, (ii) the in-gel cbb_3-Cox activity, (iii) the presence of fully assembled complex or subcomplexes in the membrane, and (iv) the presence of each subunit, including the small CcoQ subunit in the membrane. Altogether, our data suggest that CcoQ is involved in the stability of the cbb_3-Cox during its biogenesis. Moreover, the results support a sequential assembly model in which CcoQ would first associate to CcoN prior to CcoO association to form a CcoNQO 3,3′-diaminobenzidine tetrahydrochloride (DAB)-active subcomplex. CcoP is proposed to be the last subunit to assemble. Once the CcoNQOP complex is fully formed, CcoQ is released and degraded by the FtsH protease. The presence of an active CcoNOP complex in *ccoQ*$^-$ mutant demonstrated that this complex encompassed all the cofactors necessary for its function, therefore indicating that heme and copper insertions into CcoN are CcoQ-independent.

Results

cbb_3-Cox activity and expression are maximal under microaerobiosis

In an attempt to elucidate the assembly pathway of cbb_3-Cox in *R. gelatinosus*, we first examined the optimal oxygen growth conditions and monitored the activity and expression profile of cbb_3-Cox in response to oxygen level. We recorded the dissolved oxygen level in the culture medium of WT cells grown under various conditions, which reflects the oxygen consumption and oxygen reductase activity. We also addressed the contribution of cbb_3-Cox for *in vivo* oxygen consumption under microaerobiosis. In WT cells, the oxygen consumption rate was higher under microaerobiosis and slower under aerobiosis (Fig. 1*A*). Dissolved oxygen was totally consumed in WT cells grown under semiaerobiosis and microaerobiosis. In *R. gelatinosus*, two functional oxidases were identified: the *bd* quinol oxidase and the cbb_3-Cox (7). To assess the contribution of these two oxidases in oxygen consumption under microaerobiosis, we recorded the dissolved oxygen level in the culture medium of the *bd*$^-$ and cbb_3^- deletion mutants. The oxygen consumption of the *bd*$^-$ mutant was similar to that of WT. In contrast, it was severely affected in the cbb_3^- mutant. Therefore, in the *bd*$^-$ mutant, cbb_3-Cox reduced oxygen efficiently, whereas in the cbb_3^- mutant the *bd* quinol oxidase was active and responsible for the slow oxygen consumption rate. These results confirmed that cbb_3-Cox is the main oxidase involved in oxygen consumption under microaerobiosis in *R. gelatinosus*.

cbb_3-Cox in-gel activity staining was analyzed and supported the *in vivo* data. Indeed, the in-gel cbb_3-Cox activity was maximal under microaerobiosis and decreased when the oxygen level in the medium increased (Fig. 1*B*). Under photosynthesis condition, no activity was detected, which is consistent with a role of *R. gelatinosus* cbb_3-Cox only in photosynthesis initiation (7). Similarly, the level of expression of the four cbb_3-Cox subunits matched the oxidase activity profile: the amount of the four subunits (CcoN 53 kDa, CcoO 23 kDa, CcoP 32 kDa, and CcoQ 6.5 kDa) in the membrane was maximal under microaerobiosis (Fig. 1*C*).

Altogether, these data support a maximal level of expression and a central role of cbb_3-Cox for oxygen consumption under microaerobiosis. Therefore, for the study of the cbb_3-Cox assembly, the subsequent experiments were all performed under microaerobic condition.

The expression of cbb3-Cox and its CcoQ subunit is time-dependent

We also questioned whether the cbb_3-Cox activity and expression were identical with time in the WT strain after the dissolved oxygen level is null and constant. To check this, we harvested cells at different time points after oxygen level reached zero (from 0 to 35 h) for analysis. We found that cbb_3-Cox expression varied with time. cbb_3-Cox in-gel activity staining (Fig. 2*A*) and CcoN, CcoO, and CcoP amounts (Fig. 2*B*) increased up to 15 h after the oxygen level reached zero, and they decreased after 25 h in our experimental conditions. On Western blots following BN-PAGE separation, these three subunits were detected in one main band (Fig. 2*B*) and therefore

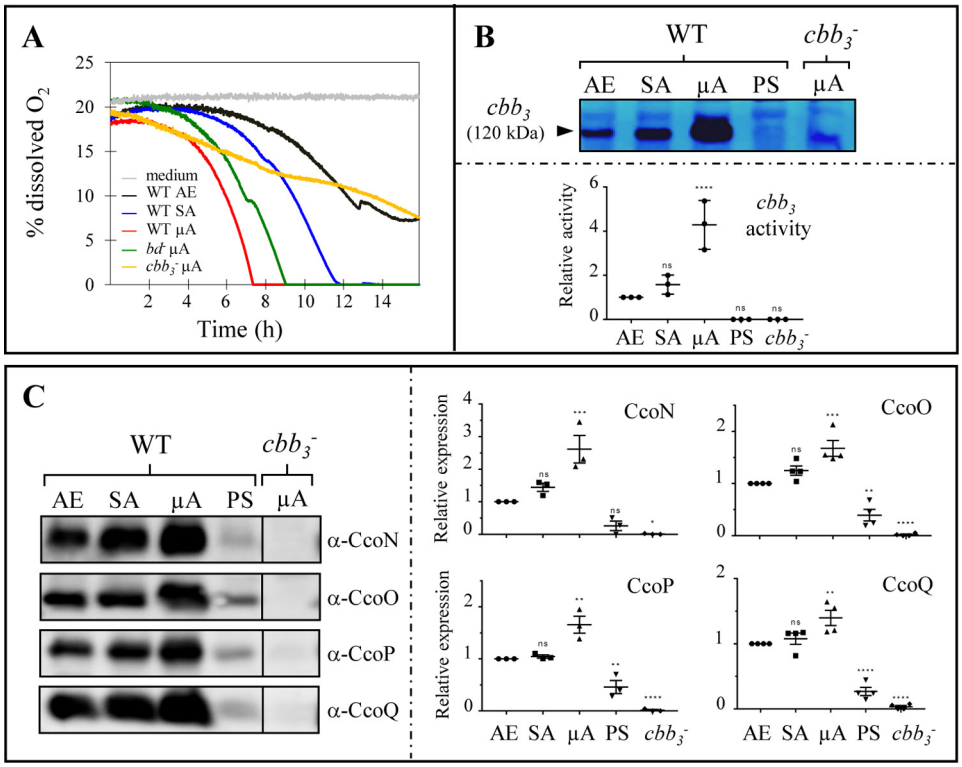

Figure 1. cbb_3-Cox expression and activity. *A*, oxygen consumption of WT, cbb_3^-, and bd^-. The WT was grown under aerobiosis (*AE*), semiaerobiosis (*SA*), or microaerobiosis (*µA*). cbb_3^- (*ccoN::Km*) and bd^- (*cydA::Ω*) mutants were grown under microaerobiosis. Non-inoculated medium was used as a control. *B*, cbb_3 oxidase in-gel activity staining of *n*-dodecyl β-D-maltopyranoside-solubilized membranes of WT grown under various conditions and cbb_3^- mutant grown under microaerobiosis. Activity was detected by 7.5–12% acrylamide gradient BN-PAGE in the presence of DAB. *PS*, photosynthesis. *C*, SDS-PAGE, Western blotting, and immunodetection of cbb_3 subunits using antibodies raised against each subunit. WT microaerobiosis- and semiaerobiosis-grown cells were harvested after 5 and 4 h at 0% O_2, respectively. Total membrane proteins were heated at 37 °C for 10 min, and 10 µg was loaded. Scatter plots demonstrating the quantitation (ImageJ) of activity or protein amount are shown. Results are the average of three to four different experiments. The quantification is shown relative to aerobic condition. The results are expressed as the mean ± S.E. (*error bars*). Significance of variation was determined by one-way ANOVA with Dunnett's multiple comparison test. ****, $p < 0.0001$; ***, $p < 0.001$; **, $p < 0.01$; *, $p < 0.1$; *ns*, non-significant.

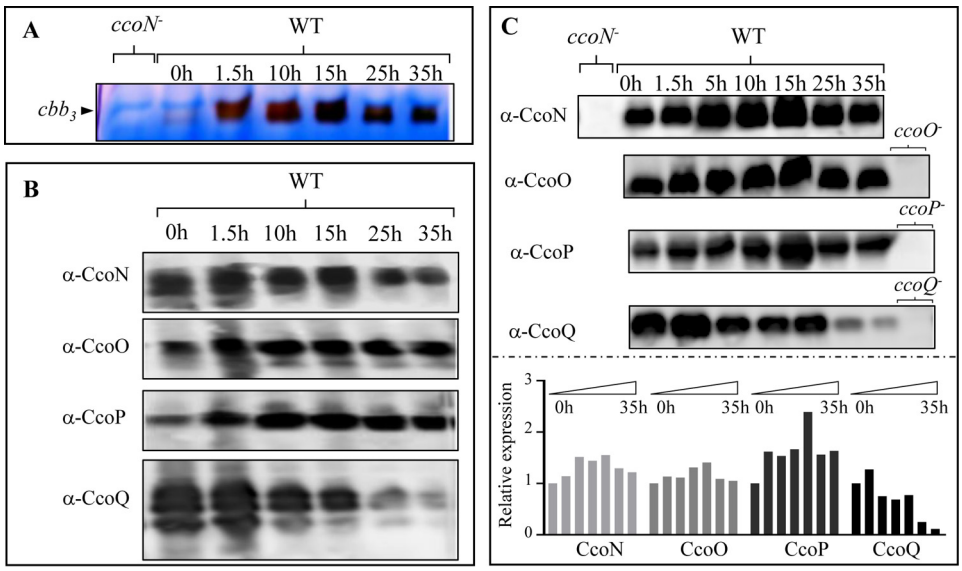

Figure 2. Microaerobic expression profile of cbb_3 at different time points. *A*, cbb_3 oxidase in-gel activity staining after BN-PAGE analysis. *B*, BN-PAGE, Western blotting, and immunodetection of cbb_3 subunits. For the detection of CcoN, the membrane was first probed with anti-CcoQ antibodies, then stripped, and reprobed with anti-CcoN antibodies. *C*, SDS-PAGE, Western blotting, and immunodetection of cbb_3 subunits. 10 µg of protein was loaded except for the membrane revealed with anti-CcoQ for which only 3.3 µg of total membranes was loaded. Membrane proteins from cbb_3 mutants were loaded as a negative control as indicated. Quantification of cbb_3 subunits levels detected by immunoblotting and showing the decrease of CcoQ was performed using ImageJ. The ratio was normalized relative to time point 0 h.

assembled in the same complex, which corresponds to the DAB-active band. Surprisingly, the expression of CcoQ was different from the other three subunits. The CcoQ amount was maximal right after the oxygen level reached zero and then underwent significant decay with time. The difference observed in the expression profile should be related to the oxygen avail-

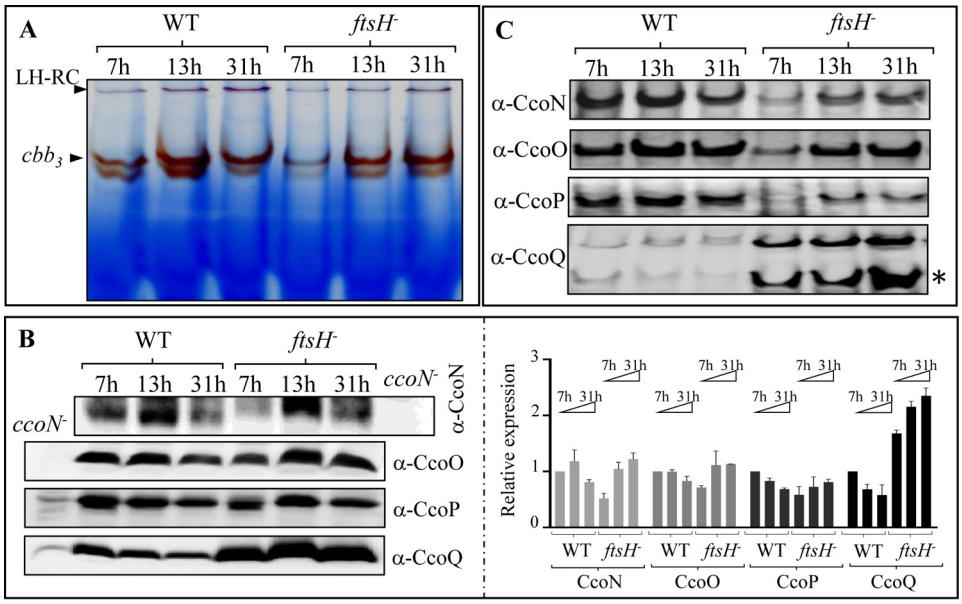

Figure 3. CcoQ accumulation in *ftsH* deletion mutant. WT and *ftsH*$^-$ cells were harvested at different times once the dissolved oxygen reached zero. *A*, cbb_3 oxidase in-gel activity staining. *B*, SDS-PAGE, Western blotting, and immunodetection of cbb_3 subunits. The membrane proteins of *ccoN*$^-$ mutant were used as a control. Quantification of cbb_3 subunits levels detected by immunoblotting showing the increase of CcoQ in *ftsH*$^-$ cells was performed using ImageJ. Results are the average of two different experiments. The quantification is shown as relative to time point 7 h. The results are expressed as the mean ± S.E. (*error bars*). *C*, BN-PAGE, Western blotting, and immunodetection of cbb_3. * indicates the low molecular weight band detected with the anti-CcoQ antibodies. *LH-RC*, light-harvesting reaction center.

ability in the medium. Indeed, at collected times 0 and 1.5 h, cells have just reached 0% of dissolved oxygen, and cbb_3-Cox was expressed at a low level. After 10 h, cells consumed very rapidly the diffusing oxygen in the medium, resulting in a net value of 0% dissolved oxygen and an increased cbb_3-Cox expression. Moreover, CcoQ was detected in at least three bands on the BN-PAGE Western blot (Fig. 2*B*), suggesting that CcoQ was present in different complexes. It is likely that the upper band correspond to the DAB-active NQOP complex. The protein composition of these three bands is addressed below (Fig. 5).

Altogether, the data showed that the dissolved oxygen concentration has to be null and constant for ~15 h to reach the maximal level of cbb_3-Cox activity in WT cells. Furthermore, the decreased CcoQ level concomitant with the increased level of the other subunits suggests that CcoQ may be required only for the early step of cbb_3-Cox assembly.

FtsH protease is involved in cbb_3 biogenesis and is required for CcoQ decay

FtsH is a membrane zinc-dependent metalloprotease involved in the quality control of unassembled membrane complexes and in modulating levels of some membrane proteins (27, 28). In WT cells, the decay of CcoQ but the increased amount of the other three subunits is intriguing. We therefore wondered whether the CcoQ level in the membranes could be modulated by FtsH. A deletion mutant of *ftsH* was constructed, and the assembly of cbb_3-Cox in the resulting *ftsH*$^-$ mutant was analyzed. The *ftsH*$^-$ mutant exhibited a reduced oxygen consumption rate of 20% compared with the WT strain. A DAB-active complex could be detected in the membrane of the *ftsH*$^-$ mutant, albeit at lower intensity compared with the WT strain (Fig. 3*A*). Most notably, immunoblot comparison of the cbb_3 subunits on SDS-PAGE in both *ftsH*$^-$ mutant and WT strain showed that CcoQ accumulated in the *ftsH*$^-$ mutant (Fig. 3, *B* and *C*), whereas in the WT strain the CcoQ amount decreased over time as also shown in Fig. 2, *B* and *C*. Similarly, accumulation of CcoQ in the *ftsH*$^-$ mutant was confirmed by immunoblotting following membrane protein separation by BN-PAGE. Indeed, an intense CcoQ signal was detected in the lower part of the Western blots in the *ftsH*$^-$ mutant membrane, which could correspond to free CcoQ released from the complex (Fig. 3*C*). These findings showed that CcoQ is degraded by FtsH protease, and this event is probably occurring when cbb_3-Cox is fully assembled into its three subunits, CcoN, CcoO, and CcoP.

Importance of each cbb_3-Cox subunit for in vivo oxygen consumption under microaerobiosis conditions

To study the importance of each cbb_3-Cox subunit, single and double mutants of *cco* genes encoding the cbb_3-Cox subunits were generated and analyzed for their *in vivo* oxygen consumption under microaerobiosis. To check for polarity effects on the expression of the downstream genes, semiquantitative RT-PCR was carried out to check the relative amount of each *cco* transcript in the single mutants. In all constructs, the transcript of the inactivated gene was absent, whereas transcripts of the other genes, including those downstream, were unaffected (Fig. S1). Under microaerobiosis conditions, the WT strain reduced oxygen at a rate of 5.8% of dissolved oxygen/h (Fig. 4*A*). The consumption rate was greatly and similarly affected in all except one mutant (*ccoQ*$^-$). Interestingly, the inactivation of *ccoQ* gene had the least severe defect, showing a reduced oxygen consumption rate of only 30% compared with the WT strain. *ccoN*$^-$, *ccoO*$^-$, *ccoP*$^-$, *ccoPQ*$^-$, *ccoOP*$^-$, and *ccoNP*$^-$ registered a rate below 1% of dissolved oxygen/h. In these mutants, the slow oxygen consumption could be accounted for by the *bd*

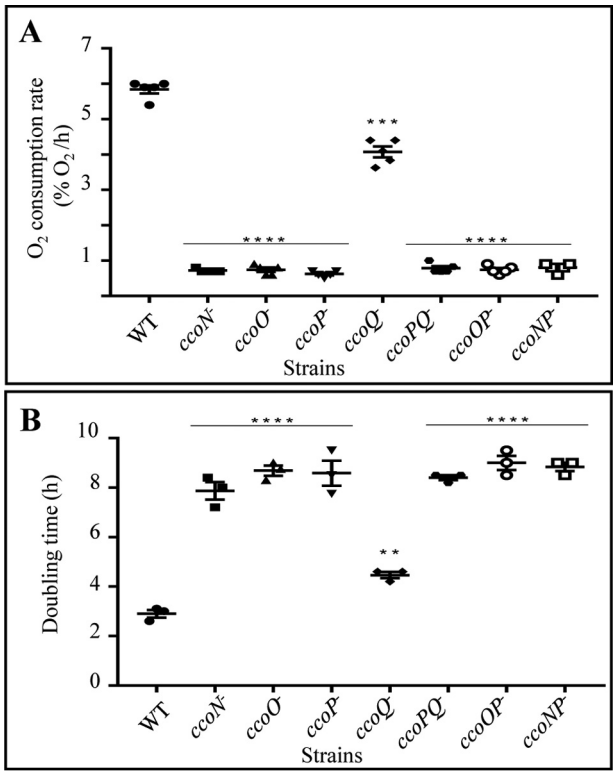

Figure 4. Importance of cbb_3 subunits for oxygen consumption. All the strains were cultivated under microaerobiosis conditions. *A*, oxygen consumption rates (percentage of dissolved oxygen/h). Results are the average of five different experiments. *B*, doubling time of WT and mutants under microaerobiosis. Results are the average of three to five different experiments. The results are expressed as the mean ± S.E. (*error bars*). Significance of variation was determined by one-way ANOVA with Dunnett's multiple comparison test. ****, $p < 0.0001$; ***, $p < 0.001$; **, $p < 0.01$.

quinol oxidase as reported previously (7). As a result, they all behaved similarly to the mutant of the catalytic subunit ($ccoN^-$). Therefore, both CcoO and CcoP subunits are essential for cbb_3-Cox activity. The reduced oxygen consumption in these mutants accounts for their higher doubling time under microaerobiosis, which reflects their slow growth (Fig. 4*B*).

CcoQ is dispensable for the assembly of cbb_3-Cox subunits within the membranes because the resulting subcomplex, CcoNOP, is fully active

All these mutant strains were also used to analyze the presence and the assembly of the remaining subunits of the cbb_3-Cox in the membrane. In fact, whether the lack of one subunit in the mutants affected the presence of the other subunits in the membrane and the formation of subcomplexes can provide data to understand the assembly process. To address this question, we checked the presence of the different subunits and putative subcomplexes in the membrane of the single and double mutants by in-gel DAB activity staining and Western blot analysis. The in-gel DAB activity staining of all the mutants was in agreement with the *in vivo* oxygen consumption data except for $ccoP^-$ mutant (Figs. 4 and 5). No in-gel DAB-active band was detected for $ccoN^-$, $ccoO^-$, and the three double mutants $ccoNP^-$, $ccoPQ^-$, and $ccoOP^-$. As expected, activity staining with the highest intensity was obtained for the WT strain (Fig. 5*A*). A band with reduced intensity and running similarly to that detected in the WT was observed for the $ccoQ^-$ mutant after extended exposure to DAB, confirming the presence of an active cbb_3-Cox in this mutant (Fig. 5*A*). This finding indicated that, in the absence of CcoQ, the other three subunits assembled correctly with copper and *b*-type hemes properly inserted into the CcoN subunit.

Similarly to $ccoQ^-$ strain, the $ccoP^-$ mutant showed a DAB-active band, which however, ran lower than the active bands found in the WT strain and $ccoQ^-$ mutant in agreement with the absence of the CcoP subunit in this subcomplex. This demonstrated that, despite the lack of CcoP, a subcomplex exhibiting a DAB activity can assemble; however, this complex is unable to reduce oxygen *in vivo* given the very low oxygen consumption rate in the $ccoP^-$ mutant. This may indicate that *in vivo*, in the process of electron transfer between the bc_1 complex and cbb_3-Cox, the soluble cytochrome *c* should interact with CcoP to shuttle electrons to CcoO and then to CcoN. This is in agreement with the structure and proposed mechanism of *P. stutzeri* cbb_3-Cox revealing that the CcoO cytochrome *c* is sandwiched between the periplasmic side of CcoN and the CcoP cytochrome *c* (12). Using the antibodies raised against the four subunits, we sought to identify the subunits that accumulate in the membrane of each mutant by separating the membrane proteins (i) in denaturing SDS-PAGE (Fig. 5*B*) and (ii) in native BN-PAGE (Fig. 5*C*) conditions. This provided the composition of the DAB-active bands and evidence of the assembly of additional, but DAB-inactive, subcomplexes within the membrane of the mutants.

Immunodetection after separation in denaturing condition of the $ccoQ^-$ mutant proteins revealed that all three subunits CcoN, CcoO, and CcoP were present in the membrane (Fig. 5*B*). Interestingly, analysis after Western blotting of the native BN-PAGE revealed a band that can be detected together with the three antibodies and would correspond to the CcoNOP DAB-active subcomplex (Fig. 5*C*). A second band that could only be detected with α-CcoN and α-CcoO antibodies was also present in $ccoQ^-$ mutant and would therefore correspond to a CcoNO inactive subcomplex. The presence of this subcomplex was further highlighted in the $ccoPQ^-$ mutant that overexpressed CcoNO (Fig. 6). Furthermore, in $ccoQ^-$ mutant membrane, CcoP was also present as a low molecular weight band and in a significant amount compared with the WT (Fig. 5*C*); this probably corresponds to free CcoP. Therefore, we concluded that two different subcomplexes were present in the membranes of the $ccoQ^-$ mutant: CcoNOP and CcoNO, corresponding respectively to the upper and lower bands detected with α-CcoN and α-CcoO antibodies following BN-PAGE separation. Given that in the absence of CcoQ the CcoNOP complex still reduced oxygen, the DAB-active band should correspond to CcoNOP subcomplex. Taken together, in agreement with the growth and oxygen consumption rates, our data demonstrated that in the absence of CcoQ an active CcoNOP subcomplex can still assemble, albeit with reduced amount and activity, and that CcoQ did not significantly impair the insertion of heme *b* and copper cofactors into CcoN subunit.

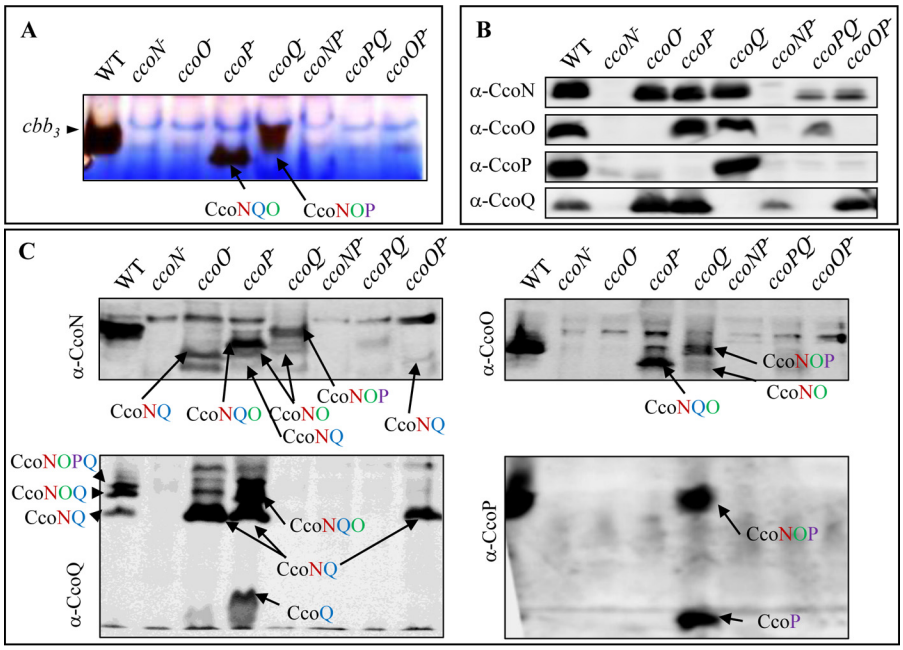

Figure 5. Importance of *cbb*$_3$ subunits for a fully active and stable complex. All strains were cultivated under microaerobiosis conditions. WT membrane of cells harvested after 15 h at 0% O_2 was used as a control. *A*, *cbb*$_3$ oxidase in-gel activity staining after overnight reaction. *B*, SDS-PAGE, Western blotting, and immunodetection of *cbb*$_3$ subunits. *C*, BN-PAGE, Western blotting, and immunodetection of *cbb*$_3$ subcomplexes. The name of the subunits of the detected subcomplexes are colored according to the assembly model scheme (Fig. 7).

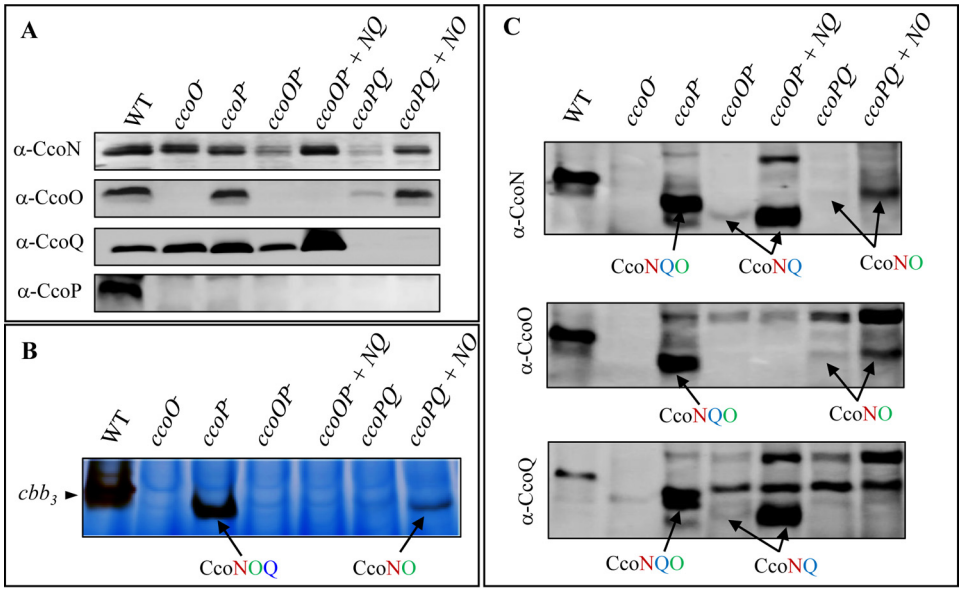

Figure 6. Detection of NO and NQ subcomplexes. All the strains were cultivated under microaerobiosis conditions. *A*, SDS-PAGE, Western blotting, and immunodetection of *cbb*$_3$ subunits. *B*, *cbb*$_3$ oxidase in-gel activity staining. *C*, BN-PAGE, Western blotting, and immunodetection of *cbb*$_3$ subcomplexes. The name of the subunits of the detected subcomplexes are colored according to the assembly model scheme (Fig. 7).

DAB-active CcoNQO and CcoNO subcomplexes can assemble even in the absence of CcoP

As mentioned previously, in the *ccoP*$^-$ mutant, a DAB-active band was detected and could correspond to either CcoNQO or CcoNO subcomplexes (Fig. 5*A*). In this mutant, the three subunits CcoN, CcoO, and CcoQ were detected on a Western blot after membrane protein separation by SDS-PAGE (Fig. 5*B*). Moreover, the Western blot of membrane separated by BN-PAGE revealed an intense band that migrated below the band detected in the WT strain with the three α-CcoN, α-CcoO, and α-CcoQ antibodies (Fig. 5*C*). This main band would therefore correspond to the CcoNQO DAB-active subcomplex. In addition, a second intense band was detected with α-CcoQ antibodies (Fig. 5*C*). This second band comigrated with the lowest of the three bands revealed in the WT membrane and was also unambiguously detected in the *ccoO*$^-$ and *ccoOP*$^-$ membranes with the α-CcoQ antibodies. Stripping of the nitrocellulose membrane to remove α-CcoQ antibodies and rehybridization with α-CcoN antibodies showed that CcoN was indeed present in the bands detected with α-CcoQ in *ccoP*$^-$, *ccoO*$^-$, and *ccoOP*$^-$ mutants (data not shown). Therefore, in the *ccoO*$^-$, *ccoP*$^-$, and *ccoOP*$^-$ mutants, the lower band detected with

α-CcoQ antibodies corresponds to the CcoNQ subcomplex. This showed that CcoN can assemble with CcoQ to form a CcoNQ subcomplex. When present, CcoO will ultimately give rise to a CcoNQO DAB-active subcomplex. To further strengthen the presence of CcoNQ subcomplex in the membrane, we overexpressed CcoNQ in the *ccoOP*$^-$ background. Membrane proteins were separated either by SDS- (Fig. 6*A*) or BN-PAGE (Fig. 6, *B* and *C*). The expression profile of the Cco subunits was analyzed along with the ability of the complexes to reduce DAB. As shown in Fig. 6*A*, overexpression of CcoNQ resulted in an increased amount of these two subunits in the membrane. On BN-PAGE, in-gel DAB activity staining did not show any active band (Fig. 6*B*). Nonetheless, a faint band was detected with α-CcoN and α-CcoQ antibodies in the *ccoOP*$^-$ membrane (Fig. 6*C*). However, a very intense band was detected in the *ccoOP*$^-$ strain overexpressing CcoNQ with the two antibodies (Fig. 6*C*), confirming the interaction between CcoN and CcoQ in the membrane. Likewise, CcoNO was overexpressed in the *ccoPQ*$^-$ background to probe for the presence of CcoNO subcomplex. Immunodetection of CcoN and CcoO after SDS-PAGE analysis confirmed their overexpression (Fig. 6*A*). Surprisingly, in-gel DAB activity staining revealed an active band in the membrane of this strain after extended exposure to DAB (Fig. 6*B*). The composition of this band was unequivocally determined by Western blot analysis after BN-PAGE separation using the α-CcoN and α-CcoO antibodies and attributed to the CcoNO subcomplex. Besides, the DAB-active CcoNO and CcoNQO subcomplexes can assemble in the absence of CcoQP and CcoP, respectively. However, none of the subcomplexes were able to reduce oxygen because the growth and oxygen consumption of *ccoQP*$^-$ and *ccoP*$^-$ strains were comparable with those of the *ccoN*$^-$ strain (Fig. 4). Taken together, these data indicated that, despite the absence of CcoQ and CcoP, CcoO can assemble with CcoN to form a DAB-active CcoNO subcomplex. However, the detection of the CcoNO active subcomplex required the overexpression of the subunits in contrast to the CcoNQO highly active subcomplex. This strongly suggests that CcoQ might guide or stabilize the binding of CcoO to CcoN to allow functional interactions.

CcoN is a required anchor, and CcoNQ is the first subcomplex to be assembled

In the *ccoN*$^-$ mutant, neither CcoQ nor CcoO could be detected, and only a trace of CcoP was present in the membrane (Fig. 5*B*). Therefore, the presence of CcoN was required for the other subunits to be present in the membrane and suggested that CcoN would act as an anchor to promote the assembly of the fully functional cbb_3-Cox in the membrane. In the absence of CcoO, both CcoN and CcoQ were present in the membrane and formed the first subcomplex, CcoNQ, as evidenced by Western blot analyses (Fig. 5, *B* and *C*). Deletion of both CcoO and CcoP (*ccoOP*$^-$ mutant) resulted in a decreased amount of CcoN and CcoQ in the membrane, suggesting that association with CcoO and CcoP would stabilize the CcoNQ subcomplex in the membrane.

CcoO is required for the association of CcoP in the late step

In the *ccoP*$^-$ strain, all three subunits CcoN, CcoO, and CcoQ accumulated in the membrane and assembled to form CcoNQ and CcoNQO subcomplexes (Fig. 5, *B* and *C*). This demonstrated that CcoP is the last partner to associate within the final complex. Analysis of the *ccoO*$^-$ strain corroborated this conclusion because only traces of CcoP were immunodetected in the membrane proteins (Fig. 5*B*). Furthermore, in the *ccoQ*$^-$ strain, the three cytochromes CcoN, CcoO, and CcoP are present and assembled to form the active subcomplex CcoNOP, thus confirming that CcoQ is not essential for the assembly and activity of cbb_3-Cox. Although CcoP is the last subunit to associate to form the active cbb_3-Cox complex, deletion of CcoP in the *ccoQ*$^-$ strain (*ccoPQ*$^-$ mutant) resulted in a decreased amount of CcoN and CcoO subunits in the membrane. The very low amount of CcoNO subcomplex detected in *ccoPQ*$^-$ strain (Figs. 5*C* and 6*C*) is in sharp contrast with the high amount of active CcoNOP in *ccoQ*$^-$ mutant and strongly suggests a role of CcoP in stabilizing the CcoNO association.

Discussion

The high oxygen affinity cbb_3-Cox are present in bacteria, including pathogens of *Pseudomonas*, *Helicobacter*, *Campylobacter*, *Neisseria*, and *Vibrio* species (29). cbb_3-Cox (CcoNQOP) are multimeric inner membrane complexes containing several cofactors; therefore, their assembly is an intricate process. So far, the assembly has been studied in very few species, as in *R. capsulatus* (2) for which a multistep and module-based assembly pathway of the cbb_3-Cox involving CcoH was proposed. CcoH is an assembly factor required for the activity and stability of cbb_3-Cox; it is present in the active complex and proposed to initiate the association of CcoNOH and CcoPQH subcomplexes (18, 26). A gene annotated as a putative *ccoH* is present in the genomes of *P. stutzeri*, *P. aeruginosa*, and *Vibrio cholerae* (Fig. S2). Nevertheless, the sequence homology of this putative CcoH with *R. capsulatus* is extremely low (16% identity and 13% homology with *P. stutzeri*) (Fig. S2), and no CcoH subunit was reported either in the purified cbb_3-Cox or in the crystal structures (12, 19). In this work, we investigated the assembly of *R. gelatinosus* cbb_3-Cox subunits by monitoring the presence of stable active or inactive subcomplexes, the importance of each cbb_3-Cox subunit for the activity, and the presence of the other subunits in the membrane. *ccoH* gene is missing in *R. gelatinosus* as well as in *H. pylori*, *N. meningitidis*, and *C. jejuni* (Fig. S3). The assembly pathway in these species might therefore be different from the module-based assembly pathway of *R. capsulatus*, involving CcoH. Indeed, our data support a sequential subunit assembly model for the cbb_3-Cox (Fig. 7) with a new role for CcoQ in the early steps. The proposed model is based on the identification of stable subcomplexes in the membrane of the WT and of a series of cbb_3-Cox mutants. We suggest that CcoQ may stabilize CcoN in the membrane and that CcoO and CcoP would be sequentially added (Fig. 7). A new finding in this work is the discharge of CcoQ from CcoNQOP. We suggest that once the active CcoNQOP complex is formed, CcoQ would be unloaded and degraded by FtsH. We propose the assembly of CcoNQ as the

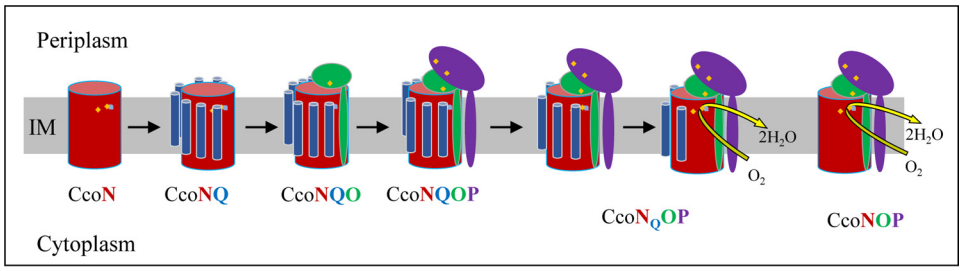

Figure 7. *cbb$_3$*-Cox assembly model and intermediate subcomplexes in the membrane. The model depicts the sequential assembly of *cbb$_3$* and the intermediates formed during this process. CcoQ could stabilize CcoN. CcoO binds to the CcoNQ complex, allowing association of CcoP. CcoQ is unloaded and degraded once the complex is fully assembled. All the depicted subcomplexes were detected either in the WT or in the appropriate mutants. The heme and copper in the isolated CcoN have not been demonstrated but seem to be independent of CcoQ attachment. The stoichiometry of CcoQ is speculative at this stage. *IM*, inner membrane.

first step of the assembly process. This is clearly different from the *R. capsulatus* model in which CcoQ was in the CcoPQH module that associates with the CcoNOH module. Indeed, we showed that CcoN and CcoQ were the only detectable subunits in *ccoO*$^-$ and *ccoOP*$^-$ mutants, and an inactive CcoNQ subcomplex was identified. Direct evidence for an interaction between CcoN and CcoQ has never been reported. Furthermore, CcoQ was not detected in the crystal structure of *cbb*$_{3\text{-}1}$ and in the crystals of *cbb*$_{3\text{-}2}$ from *P. stutzeri* (12, 19). Nevertheless, in a recent report, CcoQ was identified in these complexes, and it was suggested that CcoQ may dissociate from the CcoNQOP complex (19). The strong signal detected for CcoQ in *ccoO*$^-$ and *ccoOP*$^-$ mutants raised the question of the ratio of each subunit in the complex. A ratio of 1:1 CcoN:CcoQ is possible during maturation. However, if CcoQ stabilizes and coats CcoN subunit (12 transmembrane α-helices) in the membrane, the presence of several copies of CcoQ (one transmembrane α-helix) interacting with one CcoN molecule could also be considered. A possible role for CcoQ is to coat CcoN and to guide and assist association of CcoO to CcoN. This speculative scenario would prevent abnormal interactions between CcoN and the *c*-type cytochromes CcoO and CcoP. Similarly, the proper anchorage of CcoP to the complex requires the preassociation of CcoO to CcoN. Thus, the sequential assembly takes on full significance: the purpose is to ensure a perfect, guided assembly between the partners. In fact, in the *ccoO*$^-$ mutant, no CcoNQP subcomplex could be detected, whereas the CcoNQO complex was present in the *ccoP*$^-$ mutant. These findings demonstrated that CcoO (i) should first bind to the CcoNQ subcomplex and (ii) is required for CcoP binding (Fig. 7). The binding of CcoP after CcoNO is formed was also proposed in *R. capsulatus* and *B. japonicum* (14, 17, 18).

Our model is further supported by the identification of DAB-active CcoNQO and CcoNO subcomplexes. This is in agreement with the proposed evolution scenario of *cbb$_3$* oxidases suggesting that CcoNO form an invariable core complex to which different subunits are added (1). This sequential model is also in accordance with the crystal structure of *P. stutzeri cbb$_3$*-Cox and the relative positions of each subunit (12). In fact, the transmembrane helices of CcoO and CcoP do not fit in between those of CcoN; the soluble cytochrome *c* domain of CcoO is sandwiched between the periplasmic side of CcoN and the periplasmic soluble domain of CcoP. This structural arrangement corroborates our model in which CcoN is the backbone subunit required for CcoO and CcoP insertion. In contrast to *R. capsulatus*, no CcoPQ subcomplex could be identified in *R. gelatinosus* membrane. Finally, we also observed a decrease of the CcoQ subunit in the WT, whereas the amounts of the other subunits increased. If CcoQ was released once CcoO was assembled, then no CcoNQO complex should be detected in a *ccoP*$^-$ mutant, and the amount of CcoQ should be lower than that in a *ccoO*$^-$ mutant. However, the CcoQ level was similar in those two mutants. In *ccoP*$^-$ mutant, the major subcomplex observed was the DAB-active CcoNQO along with traces of CcoNO. However, to assemble a fully active *cbb$_3$*-Cox, CcoP should associate to CcoNQO. It is therefore conceivable that CcoP association might trigger the dissociation of CcoQ from the complex.

Conclusion

cbb$_3$ terminal cytochrome *c* oxidase is a key respiratory complex in bacteria. Taken together, our results shed light on a sequential assembly mechanism of this complex instead of the module-based pathway proposed in *R. capsulatus* and likely for CcoH-containing oxidases. Our study also highlights the importance of the interactions between the oxidase subunits during the biogenesis process as we provide evidence of the presence of at least four new active or inactive subcomplexes in the membrane. Thus, the study allowed us to identify almost all of the subcomplexes that can form in the membrane to draw a *ccoH*-independent biogenesis model that could also be effective and accurate in some pathogenic bacteria.

Experimental procedures

Bacterial strains and plasmids

Escherichia coli was grown at 37 °C on LB medium. *R. gelatinosus* was grown at 30 °C aerobically (high oxygenation; flask filled at 10th level of the total flask volume), semiaerobically (half-filled flask), or microaerobically (low oxygenation; flasks filled with the total volume of the flask) in the dark or photosynthetically in the light in filled and sealed tubes in malate medium. Antibiotics were used at the following concentrations for *E. coli* and *R. gelatinosus*: kanamycin, 50 μg/ml; ampicillin, 50 μg/ml; streptomycin, 50 μg/ml; spectinomycin, 25 μg/ml; trimethoprim, 50 μg/ml; and tetracycline, 2 μg/ml. Bacterial strains and plasmids used in this work are listed in Table 1.

Table 1
Strains and plasmids used in this work
Ap^r, ampicillin-resistant; Km^r, kanamycin-resistant; Tc^r, tetracycline-resistant; Ω, Sp^r, Sm^r, spectinomycin- and streptomycin-resistant; Tp^r, trimethoprim-resistant.

	Relevant characteristics	Source/Ref.
Strains		
E. coli JM-109	*el4$^-$ (McrA$^-$), recA1, endA1 gyrA69, thi-1, hsdR17 (rk-mk$^+$) supE44, reA1, Δ (lac-proAB) [F' traD36, proAB, lacIZΔM15*	Stratagene
R. gelatinosus strain S1	WT	34
bd$^-$	*cydA::Ω*	7
ccoN$^-$	*ccoN::Km*	7
ccoO$^-$	*ccoO::Km*	7
ccoP$^-$	*ccoP::Ω*	This work
ccoQ$^-$	*ccoQ::Km*	This work
ccoNP$^-$	*ccoP::Ω-ccoN::Km*	This work
ccoOP$^-$	*ccoP::Ω-ccoO::Km*	This work
ccoPQ$^-$	*ccoP::Ω-ccoQ::Km*	This work
ftsH$^-$	*ftsH::Tp*	This work
Plasmids		
pGEM-T	Cloning vector (Ap^r)	GE Healthcare
pUC4K	Plasmid bearing the Km cartridge (Ap^r Km^r)	GE Healthcare
pDW9	Plasmid bearing the Ω cartridge (Sp^r Sm^r)	35
p34S-Tp	Plasmid bearing the Tp cartridge (Ap^r Tp^r)	36
pBBR1MCS-3	(mob$^+$, Tc^r) expression vector	37
pBS10	pGEM-T + 1.9-kb fragment containing *ccoN*	This work
pBS11	pGEM-T + 1.56-kb fragment containing *ccoO*	This work
pBS12	pGEM-T + 2.57-kb fragment containing *ccoQ*	This work
pBS13	pGEM-T + 1.7-kb fragment containing *ccoP*	This work
pBS20	Km cartridge cloned into MscI site within *ccoN* in pBS10	This work
pBS21	Km cartridge cloned in the BsmBI site within *ccoO* in pBS11	This work
pBS24	Km cartridge cloned into XcmI site within *ccoQ* in pBS12	This work
pBS28	Ω cartridge cloned into BamHI site within *ccoP* in pBS13	This work
pSftsH	pGEM-T + 1.45-kb PCR fragment containing *ftsH*	This work
pSFtsHTp	Tp cassette cloned in MscI site of pSftsH	This work
pB3CcoNO	PCR fragment containing CcoN and CcoO under the *cco* promoter cloned into KpnI-XbaI of pBBR3-Tc	This work
pB3CcoNQO	ApaI-BamHI fragment containing CcoNQO cloned in pBBR3-Tc	This work
pB3CcoNQ	NcoI deletion of CcoO in pB3CcoNQO	This work

Measurement of dissolved oxygen during bacterial growth

Calibration and measurements were performed as advised by the manufacturer in 250-ml flasks equipped with sensor spots (30). Dissolved oxygen was measured every minute using an OXY-4 mini oxygen-sensitive minisensor (PreSens). Strains were grown under gentle shaking (140 rpm). The percentage of oxygen saturation (% O_2) was calculated using the formula: % O_2 = % air saturation × 20.95/100.

Gene cloning and plasmid construction for allele replacement

To inactivate *cco* genes in the *ccoNQOP* operon, the non-polar cassette Km was used to inactivate *ccoN*, *ccoO*, and *ccoQ* genes (Table 1). The polar cassette Ω was used to inactivate *ccoP*, the last gene of the operon. Plasmids bearing *ccoN::Km* and *ccoO::Km* were described previously (7, 25). The *ccoQ* gene was inactivated by the insertion of the Km cassette at the unique XcmI site within the *ccoQ* coding sequence. Briefly, *ccoQ* was amplified by PCR using primers ol303 (5′-GTCGGCCACGT-GCACAG-3′ and ol293 (5′-GTGTAGACCGTCTGGGG-3′) and cloned into pGEM-T. The resulting plasmid, pBS12, was subjected to XcmI restriction enzyme digestion and treated with T4 polymerase prior to ligation with the 1.2-kb EcoRI-blunt digested Km cassette conferring resistance to kanamycin to give the pBS24 plasmid. To construct a *ccoP::Ω* plasmid, the 1.7-kb fragment containing the *ccoP* gene was amplified by PCR with primers ol288 (5′-GCTGGCCAAGAACGAGGT-3′) and ol293 (5′-GTGTAGACCGTCTGGGG-3′) and cloned into pGEM-T. The resulting plasmid, pBS13, was digested with BamHI and ligated with the 2-kb Ω cartridge conferring resistance to streptomycin and spectinomycin to give the pBS28 plasmid. The plasmids pBS24 and pBS28 were used to electroporate *R. gelatinosus* WT to select the corresponding single mutants. To select the double *ccoNP$^-$*, *ccoOP$^-$*, and *ccoQP$^-$* mutants, the *ccoP$^-$* strain was used for electroporation with the pBS20, pBS21, and pBS24 plasmids, respectively. Transformants were selected on malate plates supplemented with the appropriate antibiotic under photosynthetic conditions. Following transformant selection, template genomic DNA was prepared from the ampicillin-sensitive transformants and confirmation of the presence of the antibiotic resistance marker at the desired locus was performed by PCR.

To inactivate *ftsH*, a 1448-bp PCR fragment containing the coding sequence of *ftsH* was cloned in pDRive using primers FtsH-For (5′-CAGCAAGCGCATCAAGTC-3′) and FtsH-Rev (5′-CGTTCTCGGCATAGACCATC-3′). The resulting plasmid, pSftsH, was digested with MscI to delete a 486-bp fragment and ligated with the Tp cartridge conferring resistance to trimethoprim to give the *pSftsH::Tp* plasmid.

For *ccoNO* overexpression experiments, a PCR (CcoN-KpnI, 5′-CTGCATCGTGGTACCAGTTCGAAGAC-3′ and CcoO-XbaI, 5′-TGCGGAGGGTGTCTAGATGTCCATGGT-3′) DNA fragment containing CcoN and CcoO under the *cco* promoter was cloned into KpnI-XbaI pBBR3-Tc plasmid. The pB3CcoNO was then transformed in *ccoQP$^-$* strain by electroporation. Similarly, to clone CcoNQ into pBBR3-Tc, an ApaI-BamHI fragment containing CcoNQO was cloned into pBBR3-Tc, and the result-

ing plasmid was then digested with NcoI to delete the 635-bp fragment containing the *ccoO* gene. The resulting plasmid, pB3CcoNQ, was then transformed in *ccoOP*$^-$ strain by electroporation. The presence of the plasmids in the transformants was confirmed by PCR using T7 and Rev primers flanking the cloning site of pBBR3-Tc.

Total membrane preparation

The cells were harvested by centrifugation at 6100 × *g* for 20 min at 4 °C. The cell pellet was washed after resuspension in 100 mM phosphate buffer, pH 7.5, and frozen or directly processed. Cells were lysed by two passages through a French pressure cell at 1000 p.s.i. at 4 °C in 100 mM phosphate buffer, pH 7.5, in the presence of a mixture of protease inhibitors (Roche Applied Science) and DNase (25 μg/ml). The extract was clarified by centrifugation for 30 min at 15,000 × *g* and at 4 °C. The supernatant (whole-cell extract) was centrifuged at 117,000 × *g* at 4 °C for 1.5 h. The total membrane pellet was washed in 100 mM phosphate buffer, pH 7.5, and further centrifuged as described previously. The membrane pellet was finally resuspended in 100 mM phosphate buffer, pH 7.5; fast frozen in liquid nitrogen; and then stored at −80 °C. Membrane protein concentrations were determined using the bicinchoninic acid assay (Sigma) using bovine serum albumin as a standard.

Denaturing and blue native electrophoresis

SDS-PAGE was performed according to Laemmli (31). BN-PAGE was performed as described previously (7). 2.5 mg/ml membrane proteins were solubilized in the presence of 0.25% of *n*-dodecyl β-D-maltopyranoside (Sigma), 10% glycerol (v/v), and 50 mM NaCl at 4 °C for 30 min. The solubilized membrane proteins were collected after centrifugation at 189,000 × *g* for 25 min at 4 °C and supplemented with Coomassie Blue G-250 loading buffer.

In-gel cbb_3-Cox activity

To assay cbb_3-Cox activity (in-gel DAB activity staining), BN polyacrylamide gels were incubated at room temperature in a 50 mM phosphate buffer, pH 7.5, and 8% sucrose (w/v) containing 0.31 mg/ml catalase (Sigma), 1 mg/ml horse heart cytochrome *c* (Sigma), and 0.5 mg/ml DAB. The gel was scanned at different time points during development.

R. gelatinosus cbb_3 antibody production

Antibodies raised against *R. gelatinosus* CcoN, CcoO, and CcoP were produced as described previously (32). Antibodies directed against a C-terminal synthetic peptide of CcoQ, ^{41}PFIEKDGAEASGERK^{55}, were produced in rabbits (Eurogentec). The specific peptide antibodies were further purified by a peptide-affinity column.

Western blotting and immunodetection

10 μg of total membrane protein (or 3.3 μg when specified) was separated by SDS-PAGE (12 or 15% polyacrylamide). Before loading, samples were treated for 10 min at 37 °C. Proteins were transferred to a polyvinylidene difluoride membrane (Hybond ECL PVDF membrane, GE Healthcare) in Towbin buffer containing 25 mM Tris, 192 mM glycine, 0.1% SDS (w/v), and 20% ethanol (v/v). Membranes were saturated for 1 h at 4 °C in TBST buffer (50 mM Tris, 150 mM NaCl, and 0.1% Tween 20 (v/v), pH 7.4) supplemented with 5% BSA (w/v). After five washes of 5 min in TBST buffer, the membranes were probed overnight at 4 °C with different primary antibodies: α-CcoN and α-CcoQ, 1:1000 dilution; α-CcoO and α-CcoP, 1:10,000 dilution. After five washes of 5 min in TBST buffer, the membranes were incubated for 1 h at room temperature in the presence of a secondary horseradish peroxidase (HRP)-conjugated goat anti-rabbit antibody (Bio-Rad) diluted at 1:5000. All antibodies were diluted in TBST buffer supplemented with 0.2% BSA (w/v). Reactive bands were detected using a chemiluminescent HRP substrate according to the method of Haan and Behrmann (33). Image capture was performed with a LAS-3000 charge-coupled device camera system (Fuji).

Statistical analysis

Statistical significance was determined with two-way ANOVA followed by Dunnett's multiple comparison test.

Author contributions—A. D., A.-S. S., B. K.-H., C. A., and S. O. designed research. A. D., A.-S. S., B. K.-H., M.-L. B., C. H., A. G., and S. O. performed research. A. D., A.-S. S., B. K.-H., and S. O. analyzed data. A. D. and S. O. wrote the paper.

Acknowledgments—We are grateful to Marion Babot and Sylviane Liotenberg for fruitful discussions and critical reading of the manuscript and to Thomas Chenuel for contribution to FtsH analysis.

References

1. Ducluzeau, A. L., Ouchane, S., and Nitschke, W. (2008) The cbb_3 oxidases are an ancient innovation of the domain bacteria. *Mol. Biol. Evol.* **25,** 1158–1166 CrossRef Medline
2. Ekici, S., Pawlik, G., Lohmeyer, E., Koch, H. G., and Daldal, F. (2012) Biogenesis of cbb_3-type cytochrome c oxidase in *Rhodobacter capsulatus*. *Biochim. Biophys. Acta* **1817,** 898–910 CrossRef Medline
3. Myllykallio, H., and Liebl, U. (2000) Dual role for cytochrome cbb_3 oxidase in clinically relevant proteobacteria? *Trends Microbiol.* **8,** 542–543 CrossRef Medline
4. Pitcher, R. S., and Watmough, N. J. (2004) The bacterial cytochrome cbb_3 oxidases. *Biochim. Biophys. Acta* **1655,** 388–399 CrossRef Medline
5. Preisig, O., Anthamatten, D., and Hennecke, H. (1993) Genes for a microaerobically induced oxidase complex in *Bradyrhizobium japonicum* are essential for a nitrogen-fixing endosymbiosis. *Proc. Natl. Acad. Sci. U.S.A.* **90,** 3309–3313 CrossRef Medline
6. Preisig, O., Zufferey, R., Thöny-Meyer, L., Appleby, C. A., and Hennecke, H. (1996) A high-affinity cbb_3-type cytochrome oxidase terminates the symbiosis-specific respiratory chain of *Bradyrhizobium japonicum*. *J. Bacteriol.* **178,** 1532–1538 CrossRef Medline
7. Hassani, B. K., Steunou, A. S., Liotenberg, S., Reiss-Husson, F., Astier, C., and Ouchane, S. (2010) Adaptation to oxygen: role of terminal oxidases in photosynthesis initiation in the purple photosynthetic bacterium, *Rubrivivax gelatinosus*. *J. Biol. Chem.* **285,** 19891–19899 CrossRef Medline
8. O'Gara, J. P., Eraso, J. M., and Kaplan, S. (1998) A redox-responsive pathway for aerobic regulation of photosynthesis gene expression in *Rhodobacter sphaeroides* 2.4.1. *J. Bacteriol.* **180,** 4044–4050 Medline
9. Colburn-Clifford, J., and Allen, C. (2010) A cbb_3-type cytochrome c oxidase contributes to *Ralstonia solanacearum* R3bv2 growth in microaerobic environments and to bacterial wilt disease development in tomato. *Mol. Plant Microbe Interact.* **23,** 1042–1052 CrossRef Medline
10. Jiménez de Bagüés, M. P., Loisel-Meyer, S., Liautard, J. P., and Jubier-Maurin, V. (2007) Different roles of the two high-oxygen-affinity terminal oxidases of *Brucella suis*: cytochrome c oxidase, but not ubiquinol oxidase,

is required for persistence in mice. *Infect. Immun.* **75,** 531–535 CrossRef Medline
11. Smith, M. A., Finel, M., Korolik, V., and Mendz, G. L. (2000) Characteristics of the aerobic respiratory chains of the microaerophiles *Campylobacter jejuni* and *Helicobacter pylori*. *Arch. Microbiol.* **174,** 1–10 CrossRef Medline
12. Buschmann, S., Warkentin, E., Xie, H., Langer, J. D., Ermler, U., and Michel, H. (2010) The structure of cbb_3 cytochrome oxidase provides insights into proton pumping. *Science* **329,** 327–330 CrossRef Medline
13. Kohlstaedt, M., Buschmann, S., Xie, H., Resemann, A., Warkentin, E., Langer, J. D., and Michel, H. (2016) Identification and characterization of the novel subunit CcoM in the cbb_3 cytochrome c oxidase from *Pseudomonas stutzeri* ZoBell. *MBio* **7,** e01921–15CrossRef Medline
14. Kulajta, C., Thumfart, J. O., Haid, S., Daldal, F., and Koch, H. G. (2006) Multi-step assembly pathway of the cbb_3-type cytochrome c oxidase complex. *J. Mol. Biol.* **355,** 989–1004 CrossRef Medline
15. Oh, J. I., and Kaplan, S. (2002) Oxygen adaptation. The role of the CcoQ subunit of the cbb_3 cytochrome c oxidase of *Rhodobacter sphaeroides* 2.4.1. *J. Biol. Chem.* **277,** 16220–16228 CrossRef Medline
16. Zufferey, R., Arslan, E., Thöny-Meyer, L., and Hennecke, H. (1998) How replacements of the 12 conserved histidines of subunit I affect assembly, cofactor binding, and enzymatic activity of the *Bradyrhizobium japonicum* cbb_3-type oxidase. *J. Biol. Chem.* **273,** 6452–6459 CrossRef Medline
17. Zufferey, R., Preisig, O., Hennecke, H., and Thöny-Meyer, L. (1996) Assembly and function of the cytochrome cbb_3 oxidase subunits in *Bradyrhizobium japonicum*. *J. Biol. Chem.* **271,** 9114–9119 CrossRef Medline
18. Peters, A., Kulajta, C., Pawlik, G., Daldal, F., and Koch, H. G. (2008) Stability of the cbb_3-type cytochrome oxidase requires specific CcoQ-CcoP interactions. *J. Bacteriol.* **190,** 5576–5586 CrossRef Medline
19. Kohlstaedt, M., Buschmann, S., Langer, J. D., Xie, H., and Michel, H. (2017) Subunit CcoQ is involved in the assembly of the cbb_3-type cytochrome c oxidases from *Pseudomonas stutzeri* ZoBell but not required for their activity. *Biochim. Biophys. Acta* **1858,** 231–238 CrossRef Medline
20. Hirai, T., Osamura, T., Ishii, M., and Arai, H. (2016) Expression of multiple cbb_3 cytochrome c oxidase isoforms by combinations of multiple isosubunits in *Pseudomonas aeruginosa*. *Proc. Natl. Acad. Sci. U.S.A.* **113,** 12815–12819 CrossRef Medline
21. Koch, H. G., Hwang, O., and Daldal, F. (1998) Isolation and characterization of *Rhodobacter capsulatus* mutants affected in cytochrome cbb_3 oxidase activity. *J. Bacteriol.* **180,** 969–978 Medline
22. Ekici, S., Jiang, X., Koch, H. G., and Daldal, F. (2013) Missense mutations in cytochrome c maturation genes provide new insights into *Rhodobacter capsulatus* cbb_3-type cytochrome c oxidase biogenesis. *J. Bacteriol.* **195,** 261–269 CrossRef Medline
23. Zufferey, R., Hennecke, H., and Thöny-Meyer, L. (1997) Heme C incorporation into the c-type cytochromes FixO and FixP is essential for assembly of the *Bradyrhizobium japonicum* cbb_3-type oxidase. *FEBS Lett.* **412,** 75–78 CrossRef Medline
24. Koch, H. G., Winterstein, C., Saribas, A. S., Alben, J. O., and Daldal, F. (2000) Roles of the ccoGHIS gene products in the biogenesis of the cbb_3-type cytochrome c oxidase. *J. Mol. Biol.* **297,** 49–65 CrossRef Medline
25. Hassani, B. K., Astier, C., Nitschke, W., and Ouchane, S. (2010) CtpA, a copper-translocating P-type ATPase involved in the biogenesis of multiple copper-requiring enzymes. *J. Biol. Chem.* **285,** 19330–19337 CrossRef Medline
26. Pawlik, G., Kulajta, C., Sachelaru, I., Schröder, S., Waidner, B., Hellwig, P., Daldal, F., and Koch, H. G. (2010) The putative assembly factor CcoH is stably associated with the cbb_3-type cytochrome oxidase. *J. Bacteriol.* **192,** 6378–6389 CrossRef Medline
27. Arnold, I., and Langer, T. (2002) Membrane protein degradation by AAA proteases in mitochondria. *Biochim. Biophys. Acta* **1592,** 89–96 CrossRef Medline
28. Ito, K., and Akiyama, Y. (2005) Cellular functions, mechanism of action, and regulation of FtsH protease. *Annu. Rev. Microbiol.* **59,** 211–231 CrossRef Medline
29. Pitcher, R. S., Brittain, T., and Watmough, N. J. (2002) Cytochrome cbb_3 oxidase and bacterial microaerobic metabolism. *Biochem. Soc. Trans.* **30,** 653–658 CrossRef Medline
30. Schneider, K., Schütz, V., John, G. T., and Heinzle, E. (2010) Optical device for parallel online measurement of dissolved oxygen and pH in shake flask cultures. *Bioprocess. Biosyst. Eng.* **33,** 541–547 CrossRef Medline
31. Laemmli, U. K. (1970) Cleavage of structural proteins during the assembly of the head of bacteriophage T4. *Nature* **227,** 680–685 CrossRef Medline
32. Azzouzi, A., Steunou, A. S., Durand, A., Khalfaoui-Hassani, B., Bourbon, M. L., Astier, C., Bollivar, D. W., and Ouchane, S. (2013) Coproporphyrin III excretion identifies the anaerobic coproporphyrinogen III oxidase HemN as a copper target in the Cu^+-ATPase mutant $copA^-$ of *Rubrivivax gelatinosus*. *Mol. Microbiol.* **88,** 339–351 CrossRef Medline
33. Haan, C., and Behrmann, I. (2007) A cost effective non-commercial ECL-solution for Western blot detections yielding strong signals and low background. *J. Immunol. Methods* **318,** 11–19 CrossRef Medline
34. Uffen, R. L. (1976) Anaerobic growth of a *Rhodopseudomonas* species in the dark with carbon monoxide as sole carbon and energy substrate. *Proc. Natl. Acad. Sci. U.S.A.* **73,** 3298–3302 CrossRef Medline
35. Prentki, P., and Krisch, H. M. (1984) *In vitro* insertional mutagenesis with a selectable DNA fragment. *Gene* **29,** 303–313 CrossRef Medline
36. Dennis, J. J., and Zylstra, G. J. (1998) Plasposons: modular self-cloning minitransposon derivatives for rapid genetic analysis of Gram-negative bacterial genomes. *Appl. Environ. Microbiol.* **64,** 2710–2715 Medline
37. Kovach, M. E., Phillips, R. W., Elzer, P. H., Roop, R. M., 2nd, and Peterson, K. M. (1994) pBBR1MCS: a broad-host-range cloning vector. *BioTechniques* **16,** 800–802 Medline